ARMY RESEARCH LABORATORY

AMR Magnetometer Data on Moving Military Vehicles at Aberdeen Proving Ground

by Jonathan E. Fine, Alan S. Edelstein, and David M. Hull

ARL-TR-4267 **September 2007**

NOTICES

Disclaimers

The findings in this report are not to be construed as an official Department of the Army position unless so designated by other authorized documents.

Citation of manufacturer's or trade names does not constitute an official endorsement or approval of the use thereof.

Destroy this report when it is no longer needed. Do not return it to the originator.

Army Research Laboratory
Adelphi, MD 20783-1197

ARL-TR-4267 **September 2007**

AMR Magnetometer Data on Moving Military Vehicles at Aberdeen Proving Ground

Jonathan E. Fine, Alan S. Edelstein, and David M. Hull
Sensors and Electron Devices Directorate, ARL

REPORT DOCUMENTATION PAGE

Form Approved
OMB No. 0704-0188

1. REPORT DATE *(DD-MM-YYYY)*	2. REPORT TYPE	3. DATES COVERED (From - To)
September 2007	Final	September 1999

4. TITLE AND SUBTITLE
AMR Magnetometer Data on Moving Military Vehicles at Aberdeen Proving Ground

5a. CONTRACT NUMBER

5b. GRANT NUMBER

5c. PROGRAM ELEMENT NUMBER

6. AUTHOR(S)
Jonathan E. Fine, Alan S. Edelstein, and David M. Hull

5d. PROJECT NUMBER

5e. TASK NUMBER

5f. WORK UNIT NUMBER

7. PERFORMING ORGANIZATION NAME(S) AND ADDRESS(ES)
U.S. Army Research Laboratory
ATTN: AMSRD-ARL-SE-SE
2800 Powder Mill Road
Adelphi, MD 20783-1197

8. PERFORMING ORGANIZATION REPORT NUMBER
ARL-TR-4267

9. SPONSORING/MONITORING AGENCY NAME(S) AND ADDRESS(ES)
U.S. Army Research Laboratory
2800 Powder Mill Road
Adelphi, MD 20783-1197

10. SPONSOR/MONITOR'S ACRONYM(S)

11. SPONSOR/MONITOR'S REPORT NUMBER(S)

12. DISTRIBUTION/AVAILABILITY STATEMENT
Approved for public release; distribution unlimited.

13. SUPPLEMENTARY NOTES

14. ABSTRACT
We have collected magnetic signature data on three vehicles of military interest at Aberdeen Proving Ground, MD, in September 1999 using low cost, commercial anisotropic magnetoresistance sensors. Vehicles were driven passed sensors that were located at 12 ft and 36 ft from the center of the track. The magnetic signatures that were obtained were different for the three different vehicles investigated, although some details of the signal were lost at the larger distance. The total field from the tank varied as $1/r^3$ where r is the distance between the sensor and the vehicle. The different magnetic signals generated from a tank moving backward and forward, rotating the tank's turret, and raising and lowering the tank's gun were clearly distinguishable. The signals from the tank had nearly the same values at the 12 ft and 36 ft distances, when their values were normalized by the peak values, and time axis was normalized by time interval between half-maximum amplitude points.

15. SUBJECT TERMS
AMR magnetometers, vehicle detection, magnetic signatures

16. Security Classification of:			17. LIMITATION OF ABSTRACT	18. NUMBER OF PAGES	19a. NAME OF RESPONSIBLE PERSON
a. REPORT	b. ABSTRACT	c. THIS PAGE	SAR	32	Jonathan E. Fine
Unclassified	Unclassified	Unclassified			19b. TELEPHONE NUMBER (*Include area code*) (301) 394-2357

Standard Form 298 (Rev. 8/98)
Prescribed by ANSI Std. Z39.18

Contents

List of Figures

List of Tables

INTENTIONALLY LEFT BLANK

1. Introduction

The Signal and Image Processing Division of the Army Research Laboratory is seeking to develop technology using small, low-power, low-cost sensors to detect magnetic fields in the battlefield generated by the presence and/or movement of armed troops, tracked and wheeled vehicles, and/or mines. The magnetic sensors will be part of an array of microsensors of various technologies that also include other sensor modalities such as acoustics, seismic, infrared, radio frequency (RF), and extremely low frequency electric field sensors. These sensor systems are to be deployed as unattended ground sensors (UGS) with remote activation/data acquisition as depicted in figure 1. We anticipate that multi-modal data fusion will provide enhanced detection and/or discrimination capability. We prefer sensors that can be fabricated by microelectronic/ thin film techniques that use the existing industrial base to lower cost.

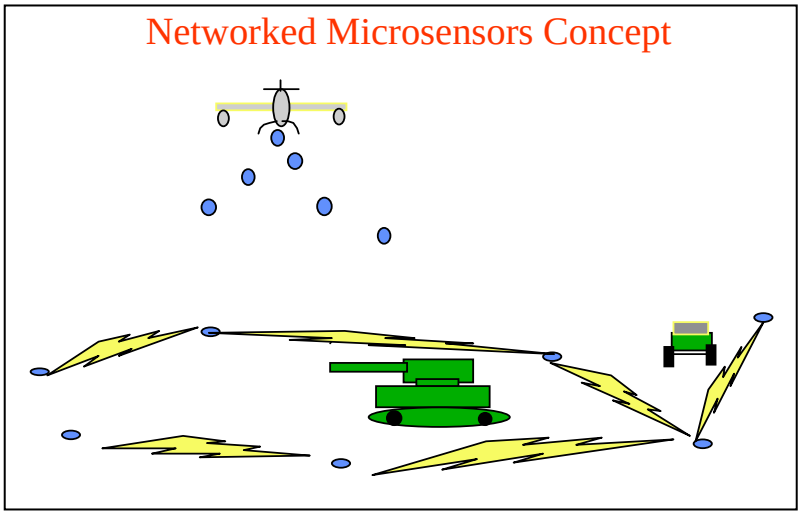

Figure 1. Networked microsensor concept showing the deployment of multiple sensors and the rf communication links between the sensors as they detect objects of military significance.

Here we report the results of an earlier test using anisotropic magnetoresistance (AMR) sensors conducted at Spesutie Island, Aberdeen Proving Ground, MD. The purpose of this testing program was to determine what useful information on vehicles of military interest could be obtained using low cost anisotropic AMR vector magnetometers. Such magnetometers may be one of the sensors employed in UGS networks. Three kinds of vehicles were investigated: a light wheeled vehicle (Vehicle A), a tank (Vehicle B), and 2 ½ ton truck (Vehicle C). We measured the difference in the signal when the tank was going forward and when it was going backward. We also investigated the signal generated by rotating the gun turret and raising and lowering the gun.

2. Magnetometers Used In Test

We used for these tests an array of four Honeywell HMR-2300, 3-axis anisotropic AMR magnetometers. The sensing element of an AMR magnetometer is a permalloy (nickel-iron alloy) thin film layer deposited on a silicon substrate.[1] The resistance due to the application of a magnetic field is about 4 percent. The material is used in a Wheatstone bridge configuration in which an applied field creates a voltage imbalance between two arms of the bridge: one being exposed to the field to be detected, and the other shielded from the field.[2] These sensor elements are manufactured on wafers and assembled with other circuit components using microelectronic fabrication techniques. We chose these magnetometers even though they have a sensitivity of only 7 nT because they are made commercially, represent the present industrial capability, and are available for about $500.00 each. As seen in figure 2 the sensor is quite small.

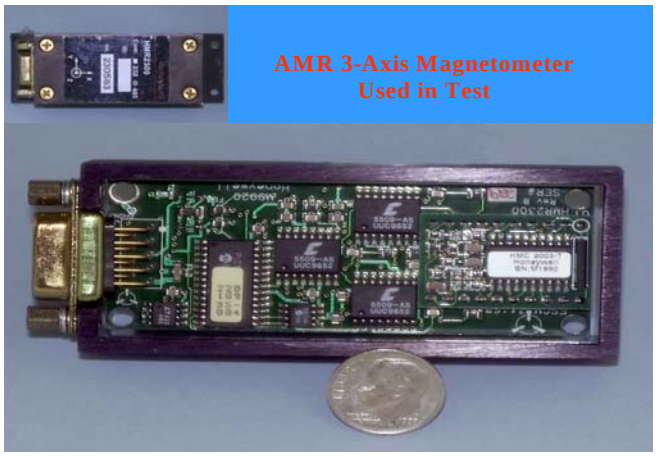

Figure 2. AMR magnetometer (HMC 2003-T) used in field test with and without its cover.

[1]Caruso, Bratland, Smith and Schneider. A New Perspective on Magnetic Field Sensing. *Proceedings of Sensor Expo* San Jose (Halmers Publishing Co.) Peterborough, New Hampshire 1998, pp 351-370.

[2]Lenz, James; Edlestein, Alan S. Magnetic Sensors and Their Applications. *IEEE Sensors Journal* **2006**, *6* (3), 635-637.

The magnetometer consists of three sensor elements positioned with their sense directions orthogonal to each other to measure the three rectangular components of an external magnetic field. Each of the sensor elements is packaged in a bridge configuration and each output is connected to a 16-Bit A/D converter. A computer records the digital outputs for storage and analysis.[3]

3. Test Instrumentation

The instrumentation block diagram that includes the four sensors used in the test is shown in figure 3. The magnetometer connects to the serial port of the computer with an RS-485 four-port isolated interface card**,** which allows simultaneous monitoring of the four magnetometers at distances up to 4,000 ft. The software interface to the computer is a National Instruments LabVIEW program. The program is compiled, and enables data collected at 20 samples per second, to be stored in a data file, and enables one of the magnetometer's outputs to be displayed graphically on the monitor as the data is being collected. The LabVIEW program attaches a time-stamp from the computer's clock to the data as it is being stored. The data Baud rate is 19,200 sec^{-1}.

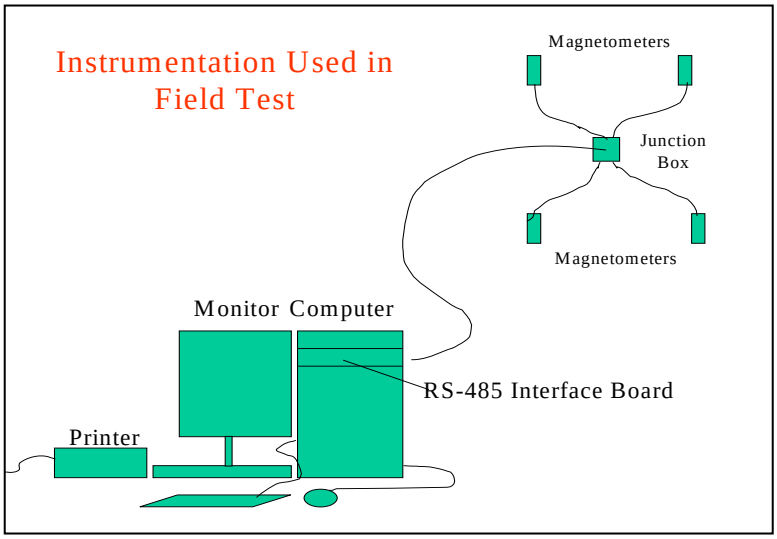

Figure 3. Diagram of instrumentation used in field test showing sensors, junction box, cables, computer, and printer.

Each HMC 2003-T magnetometer has a DB9-pin connector. Four of the pins were used: two signal leads, and two power leads. A special junction box contains 8 D-cells to provide voltage to all four magnetometers and has suitable interconnections for sending data from all four sensors back to the computer on a single 8-wire cable. This allows the power to be supplied in the vicinity (within about 30 feet) of the magnetometers, but does not require power to be

[3]Honeywell, HMR-2300 Smart Digital Magnetometer Manual.

transmitted the several hundred feet from the computer. The junction box contains four connectors wired for the magnetometers, and two connectors wired for data signals to the computer. This method allows the computer to be located in a van about 300 to 400 ft from the magnetometers. The junction box is 30 ft from the magnetometers.

4. Field Test Arrangement and Test Procedures

The test field shown in figure 4 consists of a test track, which was a dirt and gravel track about 14 ft wide and about one mile in circumference. The long direction of the track ran due north and south, and the van was located at the southern end about 100 feet from an electrical power pole. The four magnetometers were arranged in a square array as shown in figure 5. Two magnetometers were about 24 ft apart along the track and 12 ft from the center of the track. Two additional sensors were 24 ft further from the first two sensors, or 36 ft from the center of the track. There was about a 2 ft uncertainty in the position of the vehicles relative to the center of the track. The orientation of the magnetometers inadvertently was not recorded. The test procedure was to initiate recording when the vehicle started at the far end of the track and to stop when the vehicle passed out of range of the sensors.

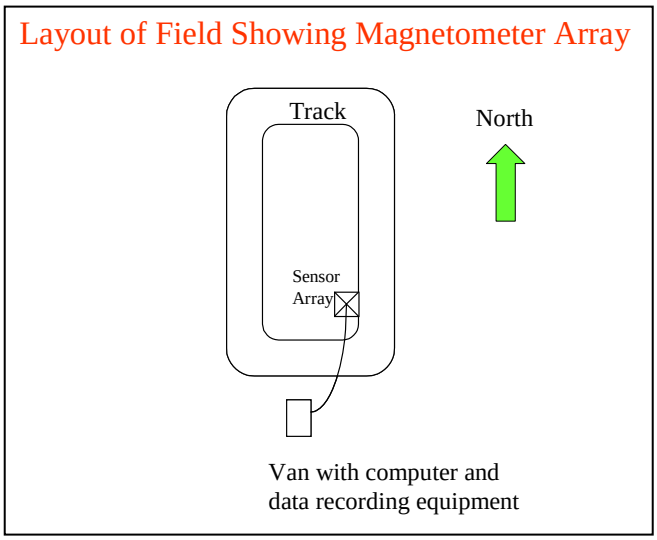

Figure 4. Layout of test field showing locations of sensor array and instrumentation van.

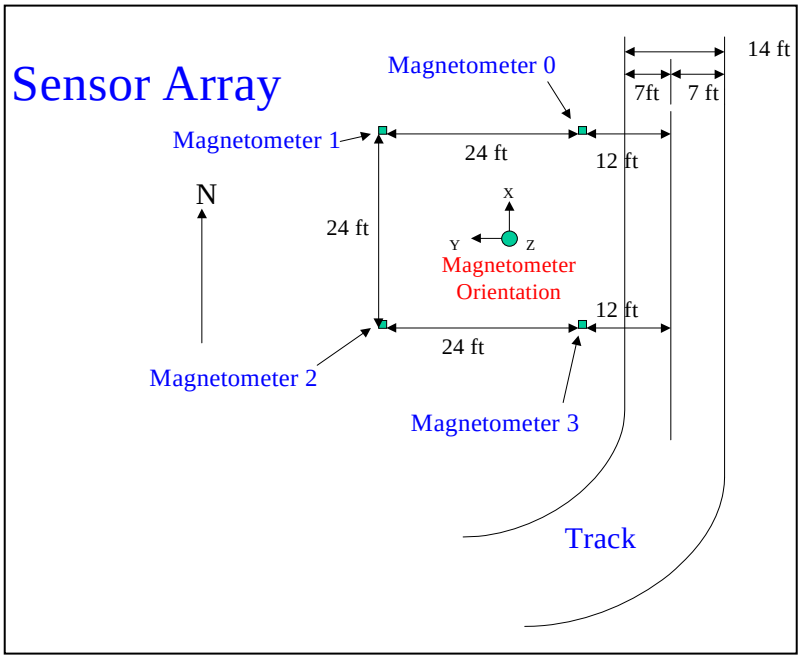

Figure 5. Arrangement of magnetometer array beside track.

5. Test Results

Distinguishing Different Vehicles

Figure 6 shows the signatures of three vehicles described earlier as they passed in succession by the magnetometer located 12 ft from the center of the track. Figures 7, 8, and 9 compare the x-, y-, and z-anomalies for the three vehicles as seen by the sensor 12 ft from the center of the track. Each vehicle has a distinct signature as compared with the other vehicles. One sees that for each axis, all three anomalies are distinct, with the tank, vehicle B, having the largest amplitude.

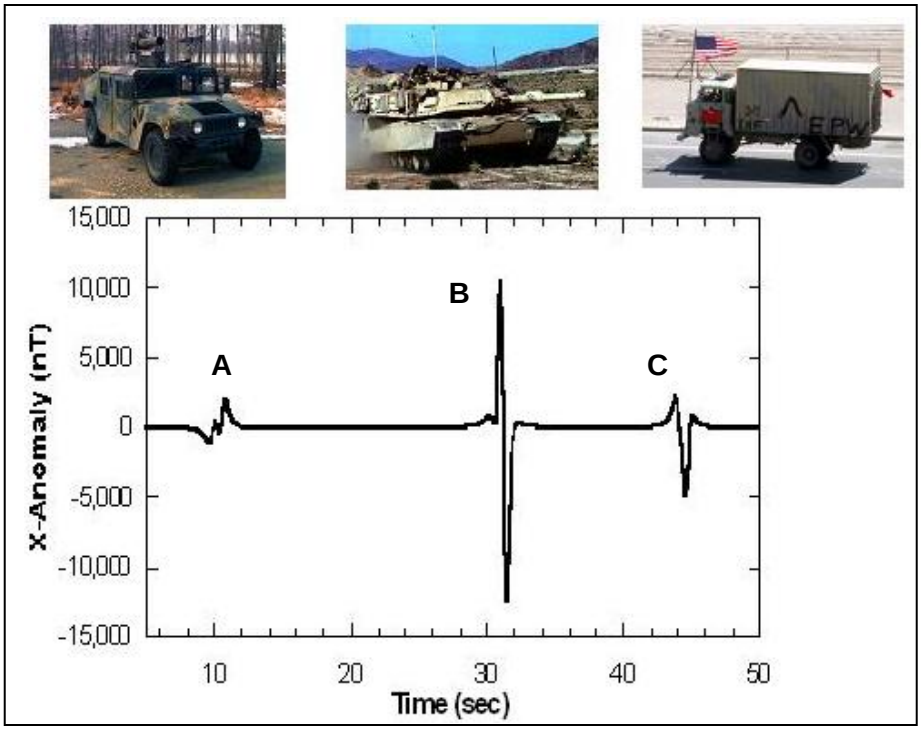

Figure 6. The x-axis signatures of a light wheeled vehicle (Vehicle A), tank (Vehicle B), and 2.5-ton truck (Vehicle C) as the vehicles passed by a sensor near the track (12 ft from center of track).

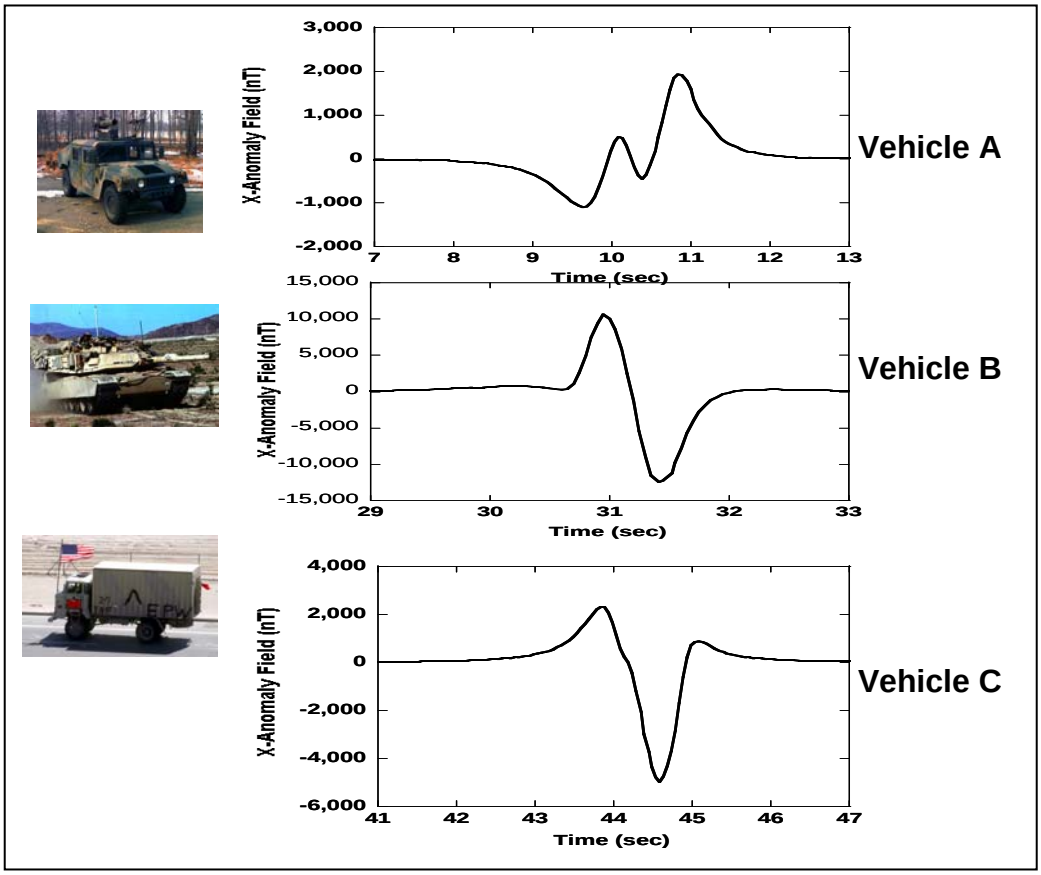

Figure 7. The x-axis signatures of all three vehicles as recorded from the magnetometer near the track (12 ft from center of track).

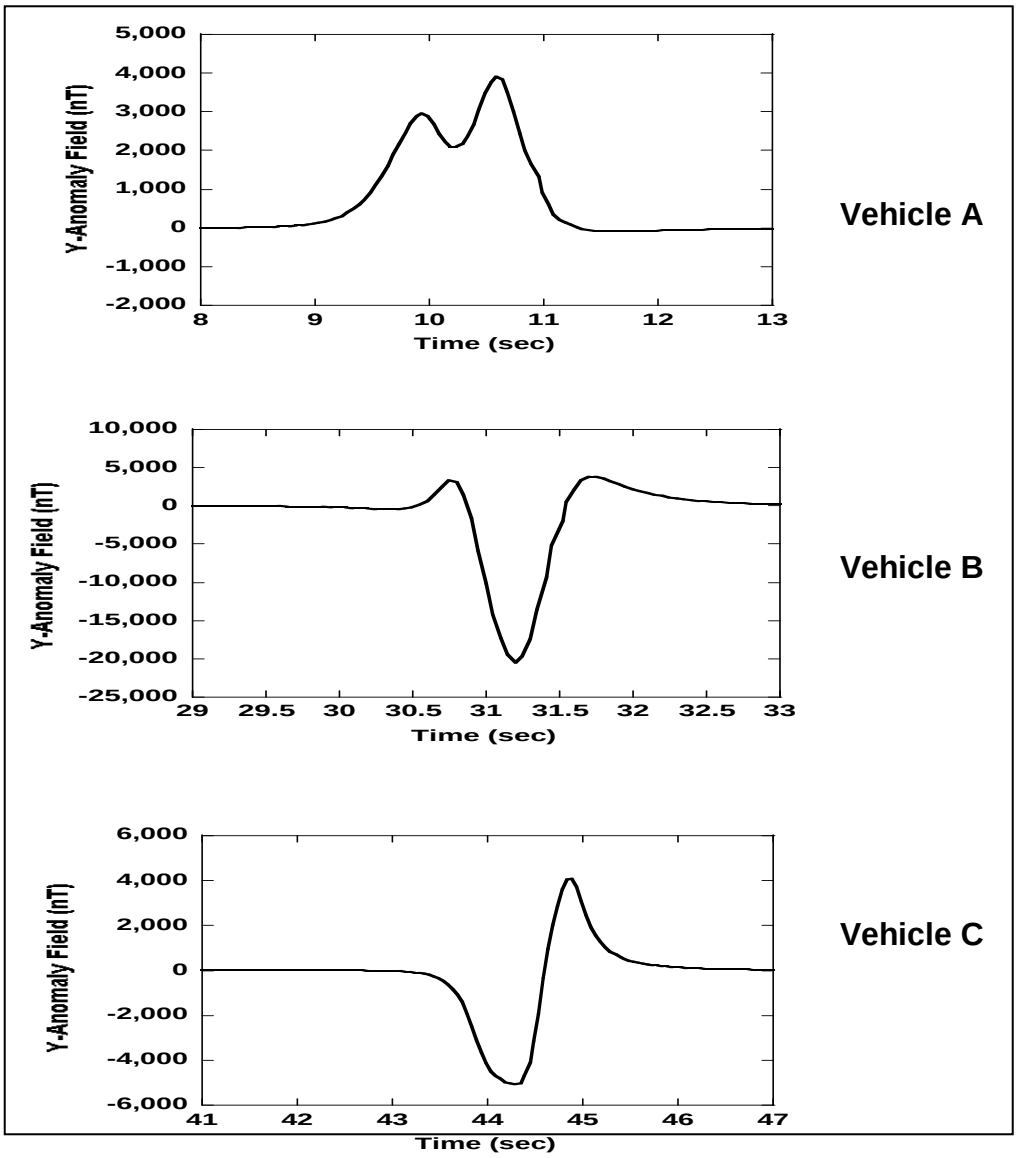

Figure 8. The y-axis signatures of all three vehicles as recorded from the magnetometer near the track (12 ft from center of track).

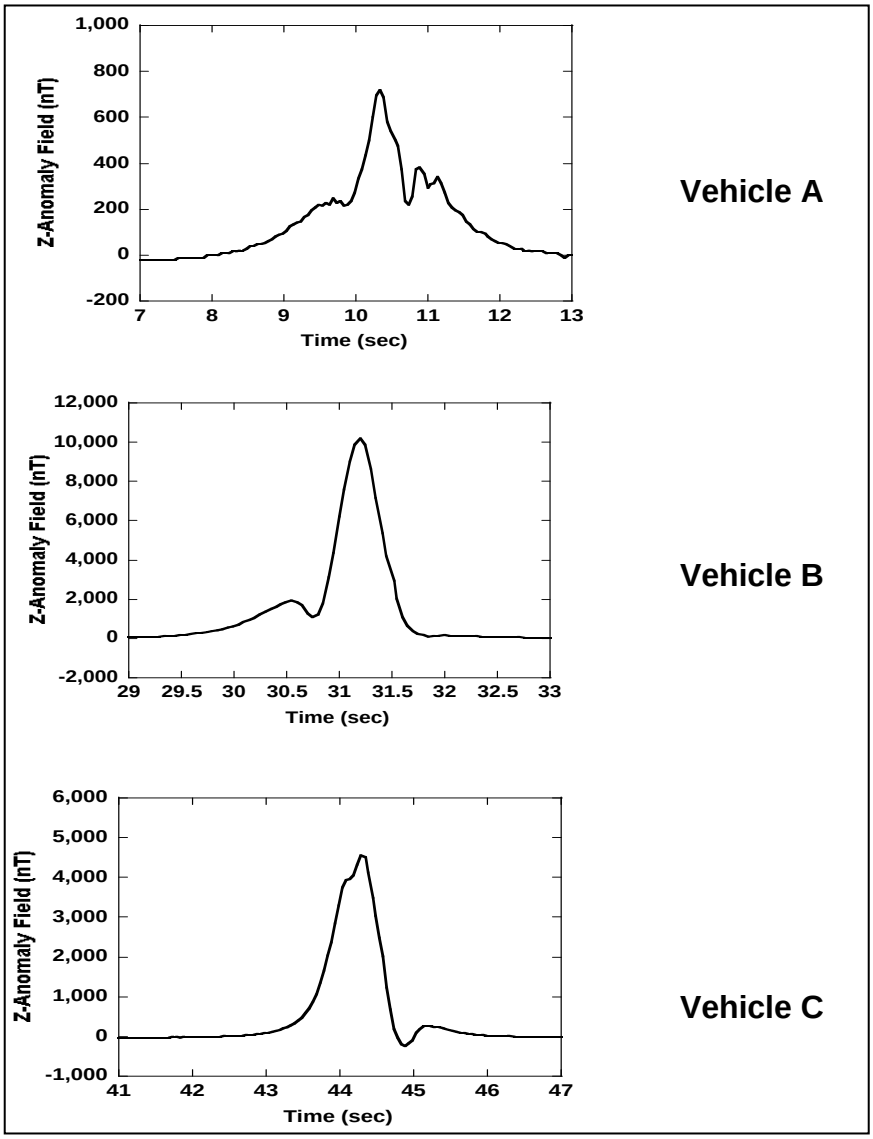

Figure 9. The z-axis signatures of all three vehicles as recorded from the magnetometer near the track (12 ft from center of track).

These distinctions disappear in the sensor 36 ft from the center of the track. This is evident in figures 10, 11, and 12 for Vehicles A, B and C, respectively. The left side of each figure shows the x-, y-, and z-axis anomaly signals for the sensor near the track, and the right side shows the corresponding signals from the sensor farther from the track. For every vehicle each axis signal from the near sensor, which is 12 ft from the center of the track, is distinct. The right side shows the same vehicle as seen by the sensor far from the track, which is 36 ft from the center of the track. (The signals from the farther sensor have been averaged over 10 data points to smooth out the bit noise, which is about 7 nT.) Note that the signal for each axis also is distinct. However,

the details detected by the close sensor cannot be seen in the data taken using the far sensor. The signals detected by the far sensor are more like a magnetic dipole.

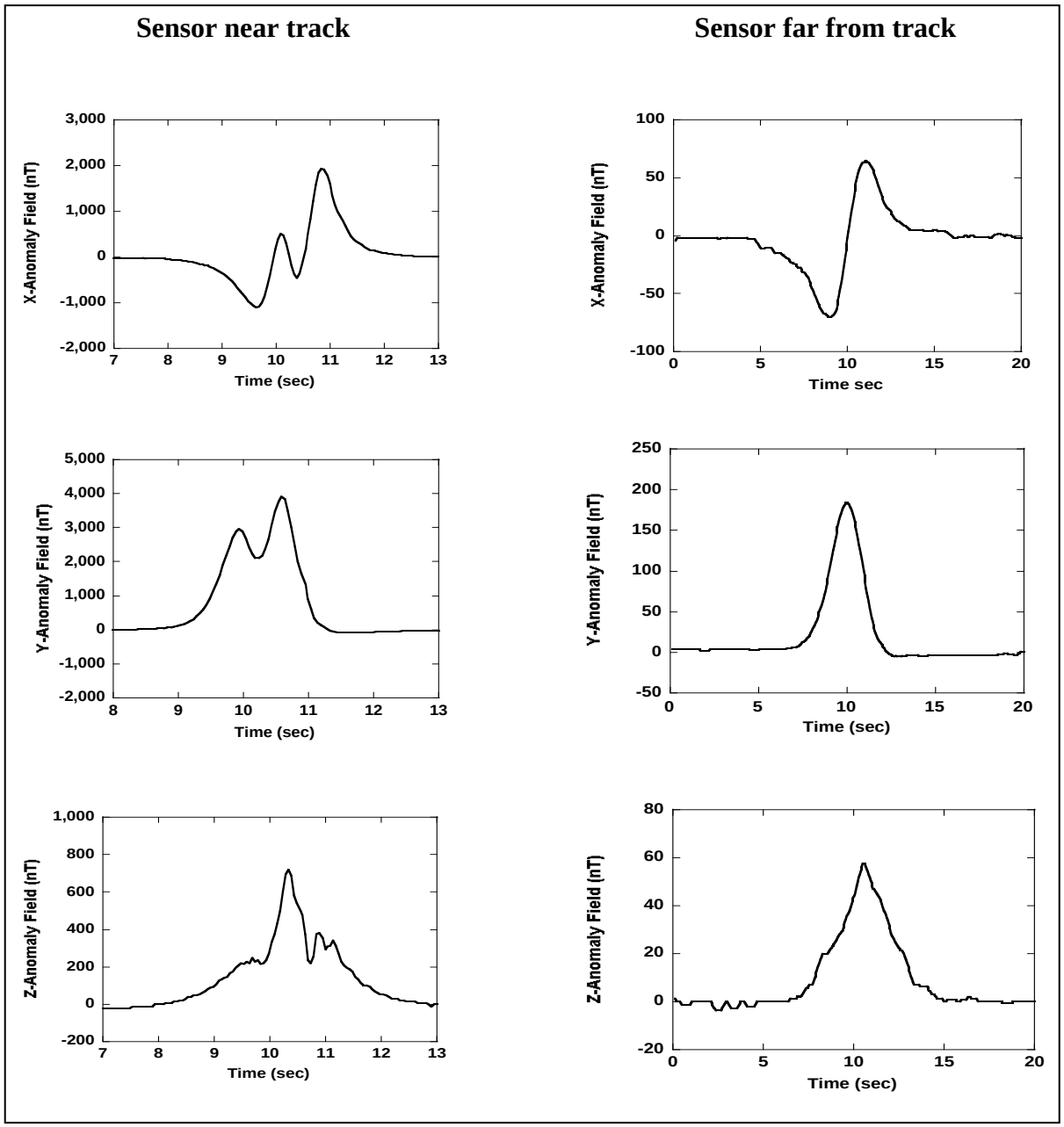

Figure 10. Vehicle A magnetic field components detected by two three-axis magnetometers: the nearer one 12 ft from the center of the track, and the farther one 36 ft from the center of the track.

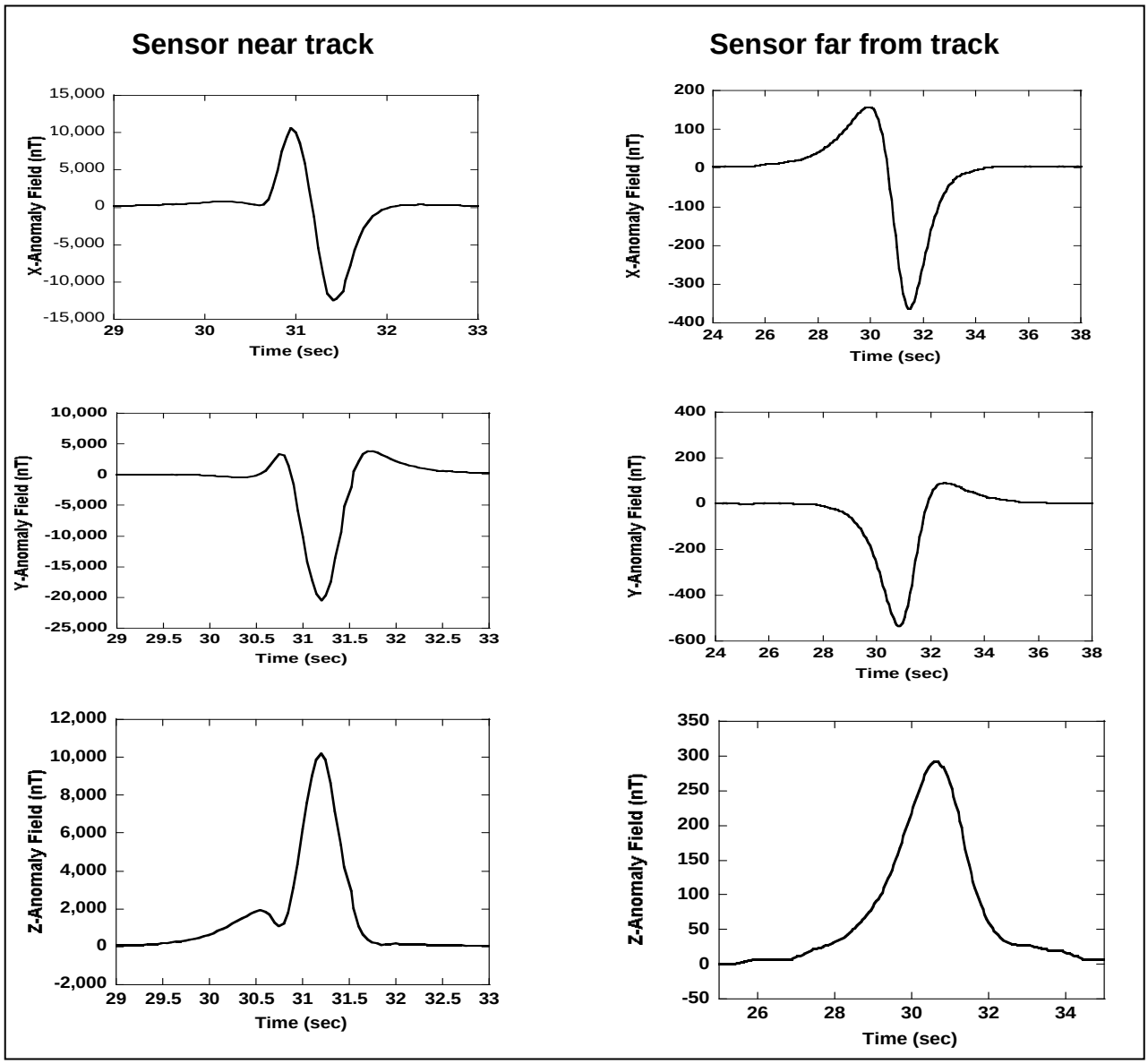

Figure 11. Magnetic field components of Vehicle B (tank) detected by two three-axis magnetometers: the nearer one 12 ft from the center of the track, and the farther one 36 ft from the center of the track.

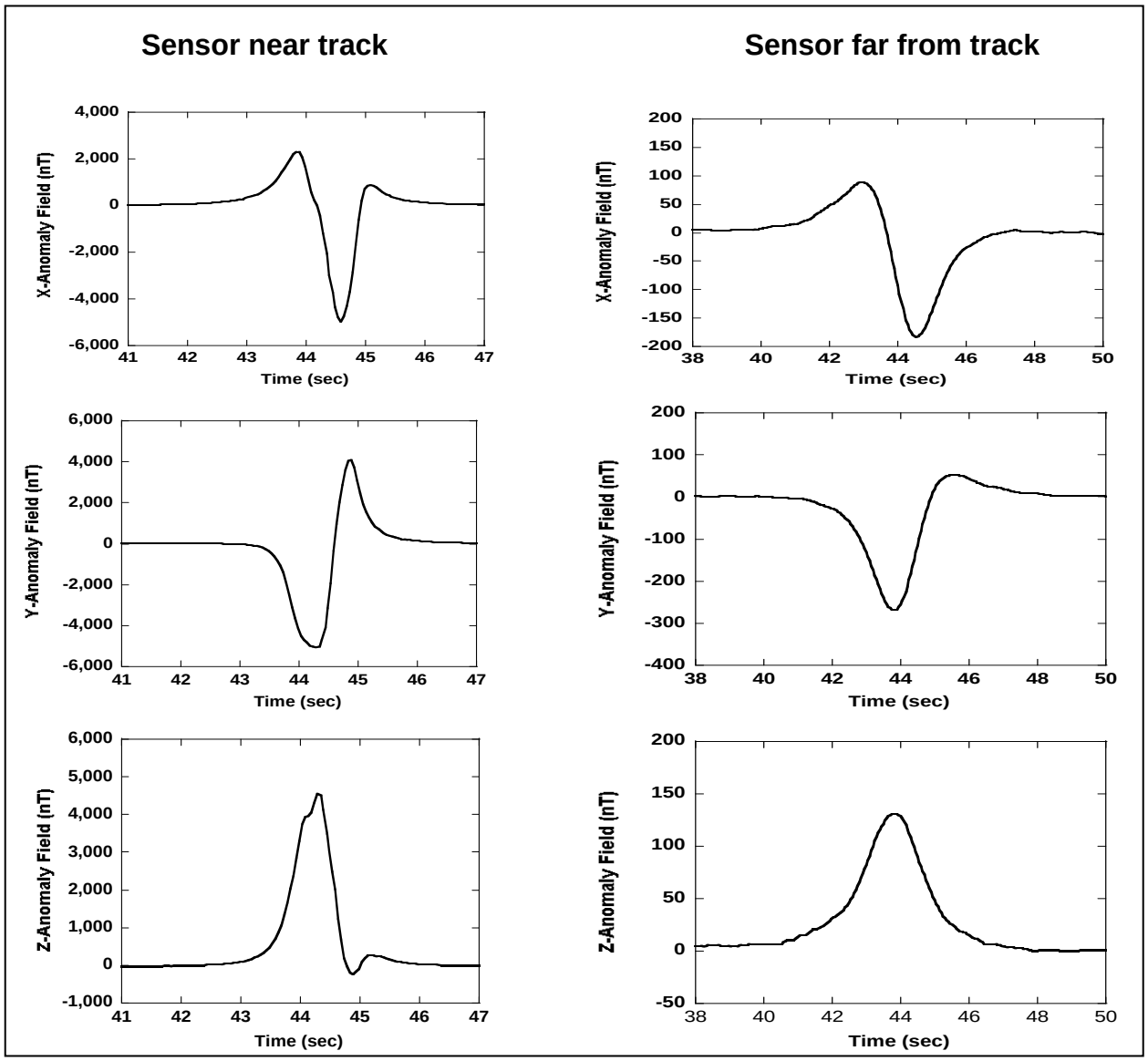

Figure 12. Magnetic field components of Vehicle C (truck) detected by two three-axis magnetometers: the nearer one 12 ft from the center of the track, and the farther one 36 ft from the center of the track.

A comparison of the right hand side of figures 11 and 12 shows that, at the far sensor, the tank and the truck are indistinguishable from each other in terms of anomaly shape, but that the tank signal has a much greater amplitude.

The significance of these results is that this UGS-appropriate technology, when comparing the vector component signals, can discriminate gross feature differences between vehicles. The component amplitudes indicate the relative magnetic size of vehicles that pass at the same distance from the sensor.

Total Field Anomaly For Sensors Near and Far From Track

The total field signal is a useful tool in obtaining information about the vehicles. The total field at each time data point is calculated as the square root of the sums of squares of the component values. The total field signals are shown in figure 13 for all three vehicles. The signals from the near sensor are on the left, and the corresponding signals from the far sensor are on the right side. The total field signal for each vehicle lacks the distinguishing shape features of the component signals and the amplitude decreases with distance from the sensor.

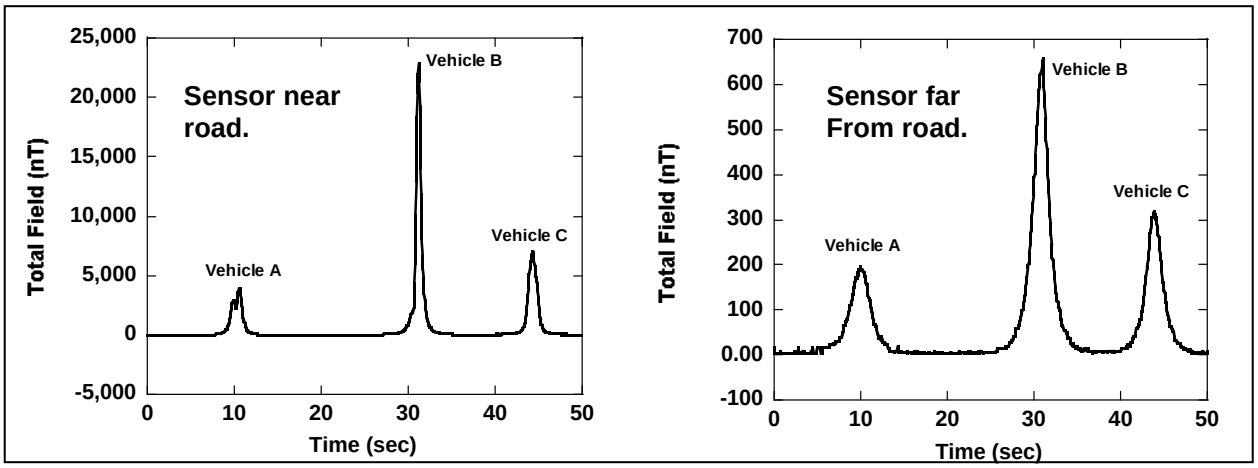

Figure 13. Comparison of Total Field of each of three vehicles for sensors near (12 ft from center of track) and far (36 ft from center of the track).

We now examine the dependence of the amplitude and signal width on distance of the sensor from the vehicle. Figure 14 shows a typical total field signal, and demonstrates the relationship between the amplitude and signal width—defined as the time difference between the two half-maximum amplitude (nT) signal points.

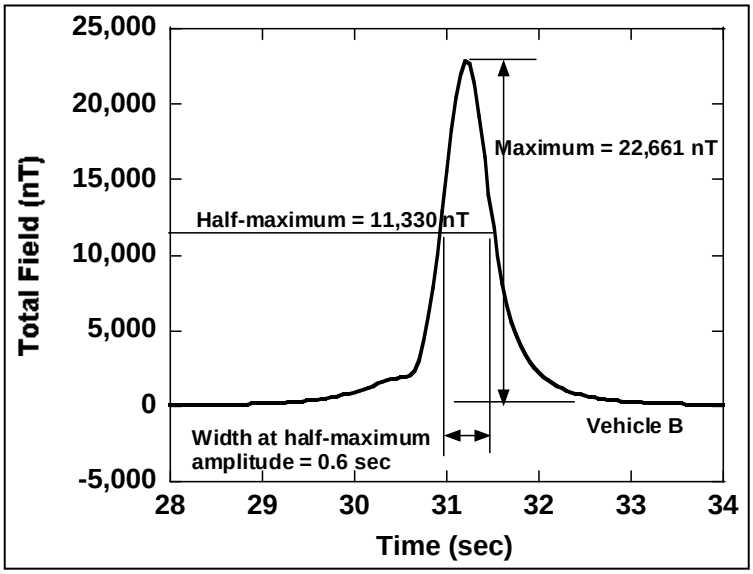

Figure 14. Total field signal from sensor near the track for Vehicle B (tank) showing the definition of signal width as the time difference between the two half-maximum amplitude (nT) signal points.

Table 1 lists the total field signal amplitude and width for all three vehicles for the sensor 12 ft from the center of the track and 36 ft from the center of the track. It also lists the cube root of the 12 ft to 36 ft amplitude ratios. The field created by a dipole at two different distances varies as the inverse cube of the sensor distance ratio. Because, in our test, the ratio of the far sensor distance to the near sensor distance is three, the cube root of the total field amplitude ratios should be three. This ratio for the three vehicles is about 3. Table 1 also shows that the signal widths are larger, and the amplitudes are smaller for the further sensor. As expected the widths are larger for the more distant sensor.

Table 1. Total field signal amplitude and width for three vehicles as seen by sensor near track and far from track.

	Maximum Signal Amplitude (nT)	**Signal Width at Half-Maximum Amplitude (sec)**	**(Ampl near/Ampl far)$^{1/3}$**
Sensor near track			
Vehicle A	3,942	1.34	2.8
Vehicle B	22,661	0.6	3.3
Vehicle C	6,949	1.16	2.8
			Average 3.0
Sensor far from track			
Vehicle A	187	2.7	n/a
Vehicle B	626	2.0	n/a
Vehicle C	319	2.1	n/a

Figure 15 shows the total field data for the tank, Vehicle B, adjusted in three ways. First, we adjusted the time axis so that the peaks occur at the same time. Second, we normalized the amplitudes of each signal to be unity at the peak. Third, we scaled the time by the time interval between the signal half-maximum amplitude points defined earlier. The two curves nearly coincide when the data is plotted in this way. At this point we are considering a dipole-like signal. In this case, the total field signal shape, when treated in this way, is independent of the separation between the target and the sensor, and may prove useful in location and tracking algorithms.[4]

The significance of these results is that the total field signal amplitude indicates the relative magnetic size of vehicles passing at the same distance of closest approach (PCA) to the sensor. The normalized and scaled total field signals are independent of sensor-target distance. These features may be helpful when the signals are used in location and tracking algorithms.

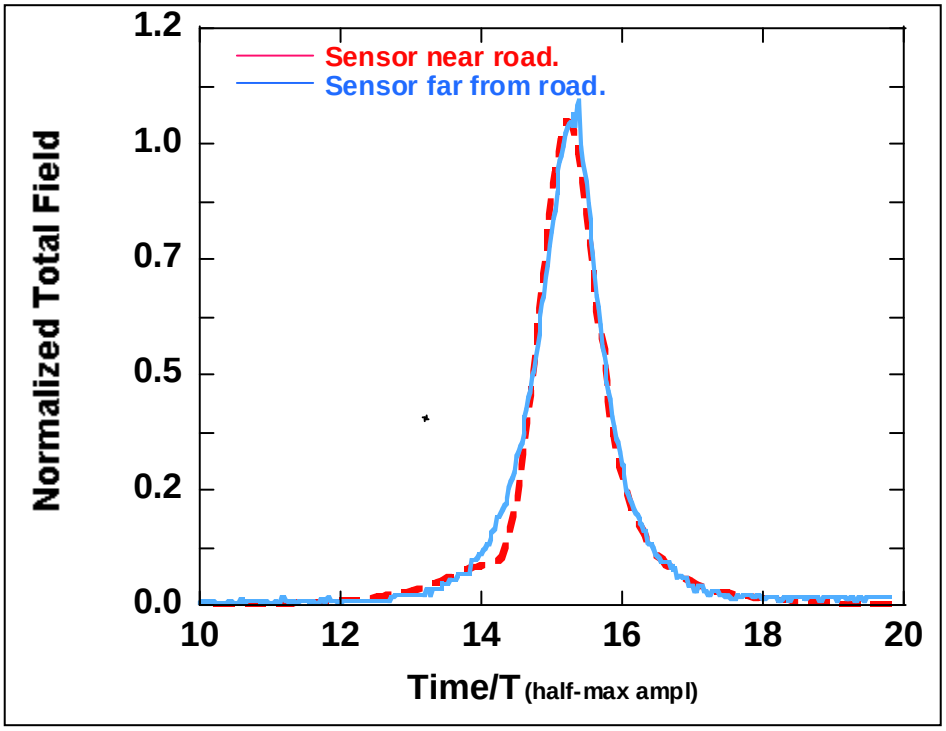

Figure 15. Similarity of total field signal shapes of Vehicle B from near and far sensors when fields are normalized with peak amplitude, and time is given in units of signal width.

[4]Edelstein. US Patent No. 6,675,123, "Magnetic Tracking Methods and Systems," June 6 2004.

Distinguishing Direction of Motion of Tank

The magnetometer near the track distinguished between the tank moving backward and forward on the track, as shown in figure 16. This figure compares the x-, y-, and z-anomalies for the tank moving backward (left column) and forward (right column). It is clear that each anomaly for backing up is the mirror image of the corresponding anomaly for going forward. The traces for moving forward are greater in amplitude and more compressed in time, probably as a result of the tank going forward faster than backing up. The differences in amplitude going forward may be due to the tank's path being slightly closer to the sensor.

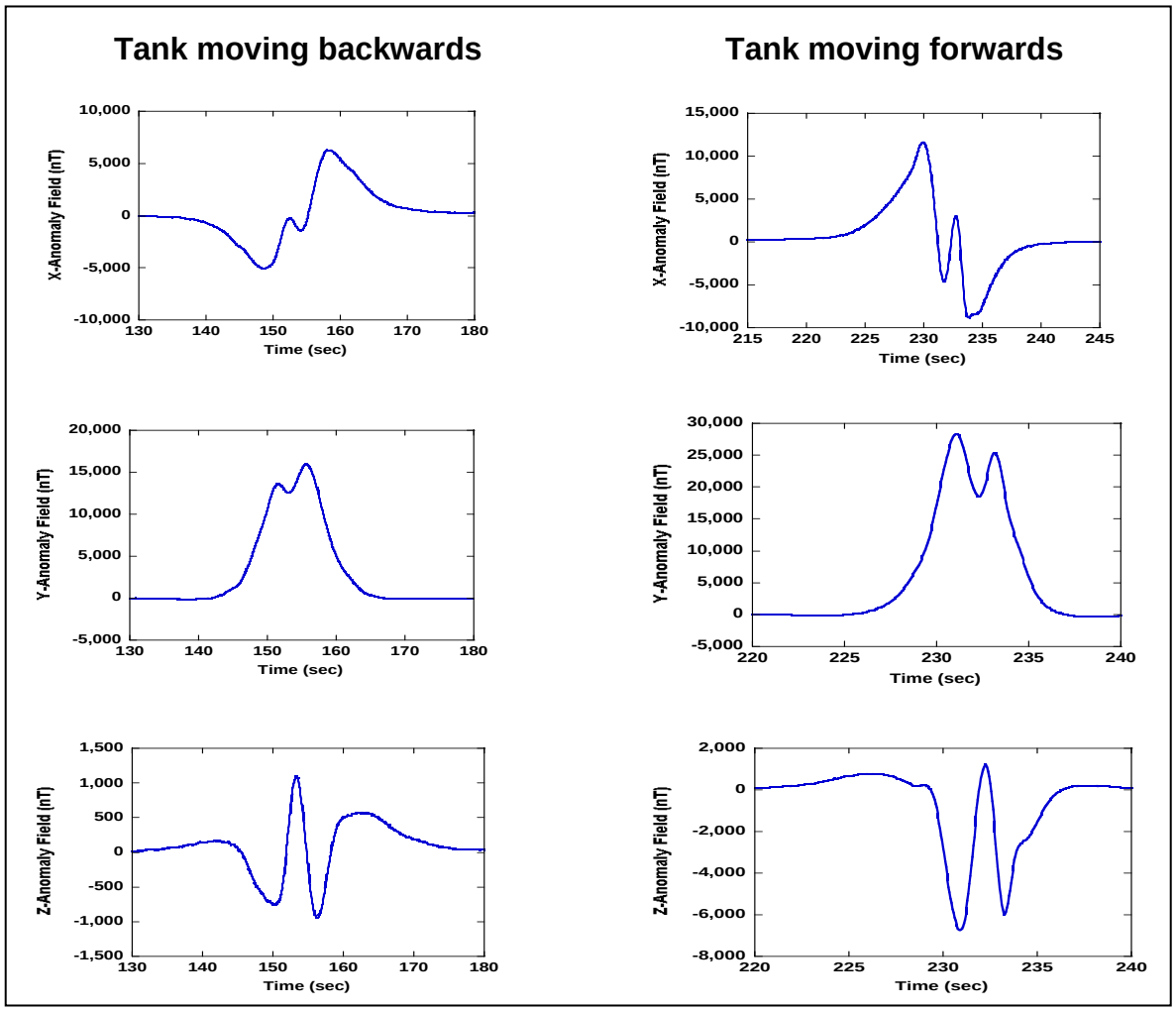

Figure 16. Comparison of x-, y-, and z-anomaly fields for tank (Vehicle B) moving backwards and then forwards on track.

Stationary Tank Rotates Turret

Figure 17 compares the anomalies for the sensor 12 ft from the track with the sensor 36 ft from the track when the stationary tank rotated its turret once. The far sensor (right side of figure 17) clearly loses details that are detected by the near sensor.

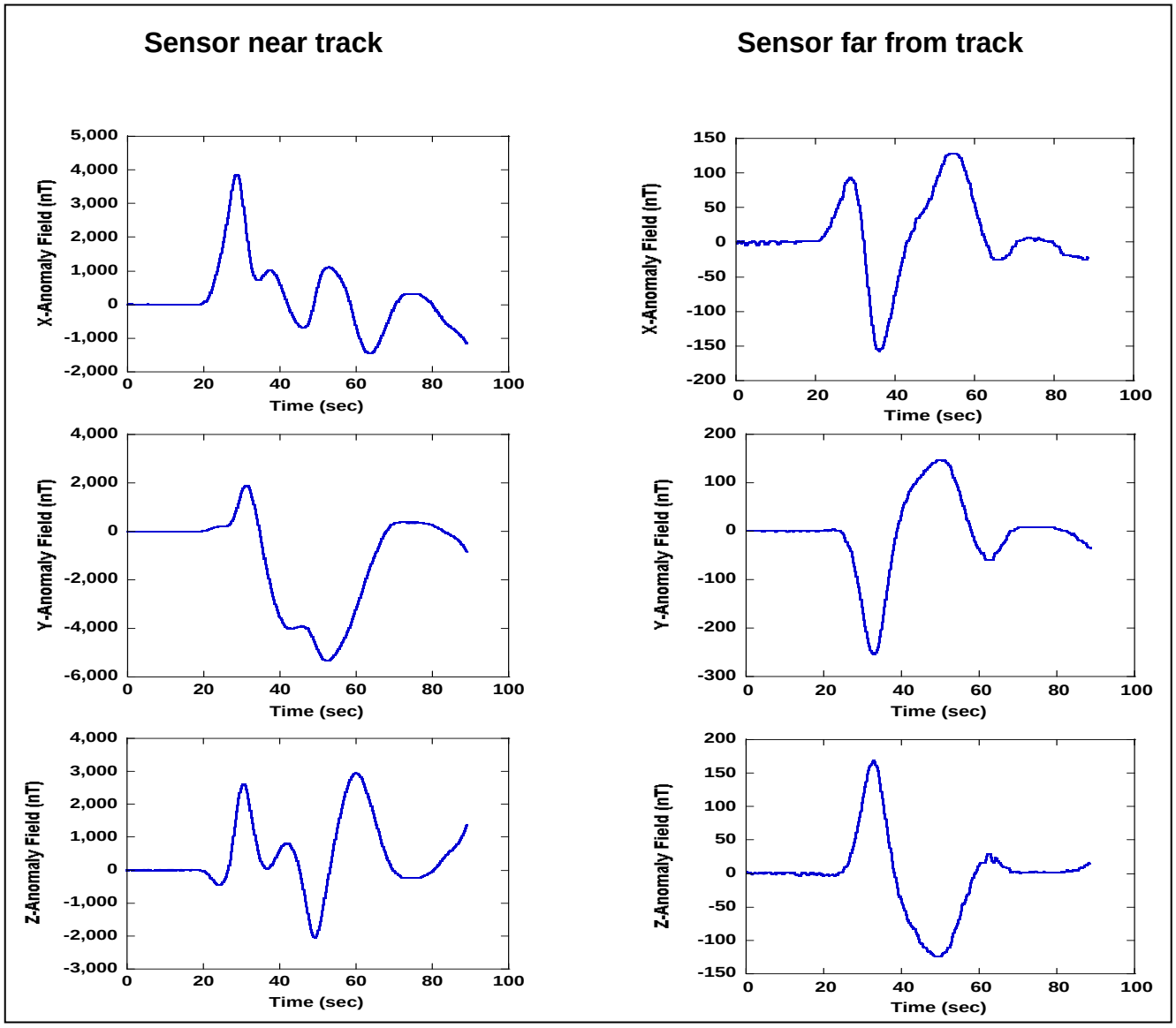

Figure 17. Comparison of x-, y-, and z-anomaly fields for tank (Vehicle B) rotating its turret as seen by sensors near (12 ft from center of track) and far (36 ft from center of the track).

Tank Raising and Lowering Gun

Figure 18 contains the x-, y-, and z-anomalies detected by the sensor 12 ft from the track when the tank is stationary and the gun is raised and lowered twice. All three traces exhibit the same oscillatory motion. The y-anomaly has the largest amplitude, about 950 nT, compared to 170 nT

for the x-anomaly and 70 nT for the z-anomaly. These results show that vector magnetometers using UGS-appropriate AMR technology can distinguish different activities of a tank.

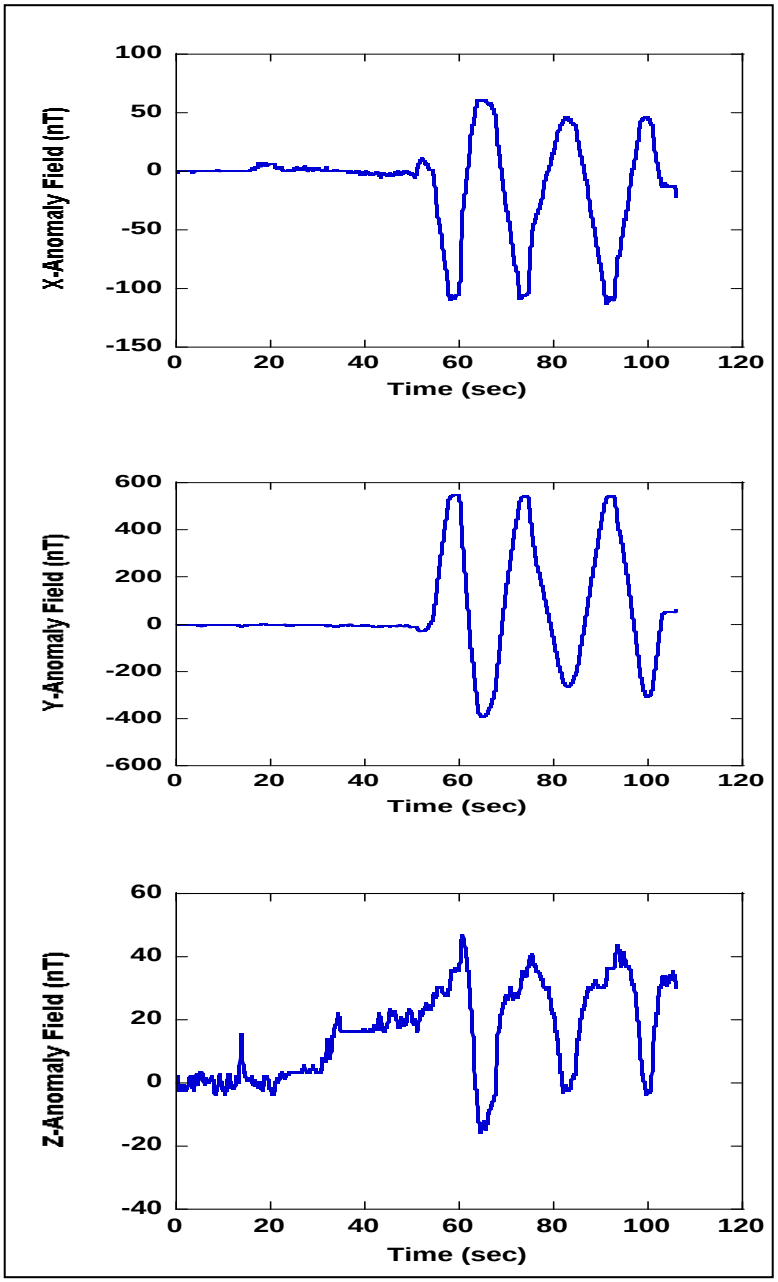

Figure 18. Comparison of x-, y-, and z-anomaly fields for stopped tank (Vehicle B) raising and lowering its gun twice as seen by sensor 12 ft from the track. These signals have been averaged over every 10 data points to smooth out the bit noise which is 7 nT.

6. Conclusions

We have presented magnetic sensor data taken with four AMR magnetoresistance sensors of three vehicles. In the case where the sensors were 12 ft from the center of the track, the vector component signals were quite different for the light wheeled vehicle, a tank, and a 2 ½ ton truck. The signals measured at 36 ft from the center of the road were approximately that of magnetic dipoles. However, the orientation of the dipole for the light wheeled vehicle was different from the orientation of the dipole of the tank and the truck. The time between when the signal was at half its maximum values was larger for the more distant sensors. One can detect when the tank's gun turret was rotated with both the sensors at 12 and 36 ft from the tank. The signal from raising and lowering the gun was smaller than the signal from rotating the gun turret and could only be detected by the sensor that was 12 ft from the tank. The signals detected at 12 ft and 36 ft from the tank had the same shape when the amplitudes and times were scaled. For all vehicles tested, the ratio of the cube root of the signal of the sensor near the track to that of the sensor far from the track approximately equals 3, as expected for the dipole model. When the total field signal is normalized by the maximum detected field, and the times are expressed in terms of the signal width at half-maximum field, the detected total field signal shape is independent of the distance between the sensor and the target.

When the total field signals from each sensor are normalized by the maximum detected field, and the times are expressed in terms of the signal width at half-maximum field, the detected total field signal shape is identical for a sensor near the target and a sensor further away. The signal shape when modified in this manner is positive, has a clearly-defined peak, and is independent of the target speed, shape or distance from the sensor. This modified total field signal (normalized field amplitude versus scaled time) when considered in conjunction with the usual signal (field amplitude versus time) may be useful in target location and detection algorithms. The results reported on here indicate that low cost AMR magnetic sensors appropriate for use in UGS networks can provide information useful in classifying target vehicles, distinguishing some vehicle activities, and estimating vehicle magnetic size.

INTENTIONALLY LEFT BLANK

Distribution List

ADMNSTR
DEFNS TECHL INFO CTR
ATTN DTIC-OCP (ELECTRONIC COPY)
8725 JOHN J KINGMAN RD STE 0944
FT BELVOIR VA 22060-6218

DARPA
ATTN IXO S WELBY
ATTN TECHL LIB
3701 N FAIRFAX DR
ARLINGTON VA 22203-1714

DEFNS INTLLGNC AGCY
ATTN RTS-2A TECHL LIB
WASHINGTON DC 20301

OFC OF THE SECY OF DEFNS
ATTN ODDRE (R&AT)
THE PENTAGON
WASHINGTON DC 20301-3080

ARMY TACOM-ARDEC
ATTN B PELTZER
BLDG 407
PICATINNY ARSENAL NJ 07806

US ARMY TRADOC
BATTLE LAB INTEGRATION & TECHL
DIRCTRT
ATTN ATCD-B
10 WHISTLER LANE
FT MONROE VA 23651-5850

CECOM NVESD
ATTN TECHL LIB
FT BELVOIR VA 22060-5806

US MILITARY ACDMY
MATHEMATICAL SCI CTR OF
EXCELLENCE
ATTN MAJ J HARTKE
PHOTONICS CENTER
WEST POINT NY 10996-1786

OFC OF THE PROJ MGR FOR MINES,
COUNTERMINES, & DEMLTN
ATTN AMCPM-DSA-MCD T HOFFMAN
PICATINNY ARSENAL NJ 07806-5000

OFFICE OF THE PROJECT MANAGER
FOR CLOSE COMBAT SYSTEMS
ATTN SFAE-AMO-CCS
R ANDREJKOVICS
BLDG 183
PICATINNY NJ 07806-5000

REDECOM ARDEC
ATTN TECH LIB
BLDG 59
PICATINNY ARSENAL NJ 07806-5000

SMC/GPA
2420 VELA WAY STE 1866
EL SEGUNDO CA 90245-4659

US ARDEC
ATTN AMSRD-AAR-HEP-A M HOHIL
BLDG 407
PICATINNY ARSENAL NJ 07806-5000

US ARMY ARDEC
ATTN AMSRD-AAR-AEP-S
R T KINASEWITZ
BLDG 353N
PICATINNY ARSENAL NJ 07806-5000

US ARMY INFO SYS ENGRG CMND
ATTN AMSEL-IE-TD F JENIA
FT HUACHUCA AZ 85613-5300

US ARMY NATL GROUND INTLLGNC CTR
ATTN IANG-CE-MA D C LOYD
ATTN IANG-CE-MA MS404
A GRACHES
ATTN IANG-CE-MA MS404
J N MONROE JR
2055 BOULDERS RD
CHARLOTTESVILLE VA 22911-8318

COMMANDER
US ARMY RDECOM
ATTN AMSRD-AMR W C MCCORKLE
5400 FOWLER RD
REDSTONE ARSENAL AL 35898-5000

US ARMY RDECOM CERDEC NVESD
SCI & TECHLGY DIV COUNTERMINE TECHLGY BR
ATTN AMSRD-CER-NV-ST-CMT
I MCMICHAEL
10221 BURBECK RD
FT BELVOIR VA 22060-5806

US ARMY RSRCH LAB
ATTN AMSRD-ARL-CI-OK-TP TECHL LIB T LANDFRIED
BLDG 4600
ABERDEEN PROVING GROUND MD 21005-5066

US ARMY TANK-AUTOMTV R&D CTR
ATTN DRSTA-TSL TECHL LIB
WARREN MI 48397-5000

US ARMY TROOP SUPPORT CMND
NATICK RSRCH DEV & ENGRG CTR
ATTN STRNC-MIL TECHL LIB
NATICK MA 01760-5040

NAV AIR WARFARE CTR
ATTN O ALLEN
22347 CEDAR POINT RD B2185 S1100 UNIT 6
PATUXENT RIVER MD 20670-1161

NAV RSRCH LAB
ATTN 5220 TECHL LIB
4555 OVERLOOK AVE SW
WASHINGTON DC 20375-5320

NAV SURFC WARFARE CTR
ATTN CODE B60 TECHL LIB
17320 DAHLGREN RD
DAHLGREN VA 22448-5100

NAV UNDERWATER SYS CTR
ATTN CODE 5B331 TECHL LIB
NEWPORT RI 02840

NAVAL SURF WARFARE CTR
ATTN T CLEM
6703 W HWY 98
PANAMA CITY FL 32407

NSWC DAHLGREN DIV
ATTN R BRANNON
17320 DAHLGREN RD
DAHLGREN VA 22448

NSWC/CD
ATTN D PUGSLEY
WEST BETHESDA MD

AIR FORCE ARMAMENT LAB
ATTN AFATL DLIW TECH LIB
EGLIN AFB FL 32542

BAE SYSTEMS
ATTN J SLEDGE
PO BOX 1898
EGLIN AFB FL 32542

US AIR FORCE
ATTN 46TS/OGEE T DULLE
ATTN 46TS/OGEE W TERRELL
101 E DAYTONA RD BLDG 85
EGLIN AFB FL 32542

US GOVERNMENT PRINT OFF
DEPOSITORY RECEIVING SECTION
ATTN MAIL STOP IDAD J TATE
732 NORTH CAPITOL ST., NW
WASHINGTON DC 20402

THE JOHNS HOPKINS UNIV APPLD PHYSIC LAB
ATTN TECHL LIB
JOHNS HOPKINS RD
LAUREL MD 20707

UNIV OF MARYLAND
ATTN ENGRG & TECHL LIB
RM 2168 ENGRG CLASSROOM BLDG
COLLEGE PARK MD 20742-5121

GE INFRASTRUCTURE SECURITY
ATTN P CZIPOTT
SAN DIEGO CA

LAB FOR PHYSICAL SCIENCES
ATTN A J LEYENDECKER, PH.D.
SENIOR SCIENTIST
8050 GREENMEAD DR
COLLEGE PARK MD 20740

SOUTHWEST RSRCH INST
ATTN S CERWIN
6220 CALEBRA RD
SAN ANTONIO TX 78238

SRI INTRNTL PROPULSION SCI DIV
ATTN TECHL LIB
333 RAVENWOOD AVE
MENLO PARK CA 94025-3493

US ARMY RSRCH LAB
ATTN M KILGORE
ABERDEEN PROVING GROUND MD 21005

US ARMY RSRCH LAB
ATTN AMSRD-ARL-WM-BF G HAAS
ABERDEEN PROVING GROUND MD 21005-5067

US ARMY RSRCH LAB
ATTN AMSRD-ARL-WM-BF
W OBERLE
BLDG 390
ABERDEEN PROVING GROUND MD 21005-5067

DIRECTOR
US ARMY RSRCH LAB
ATTN AMSRD-ARL-RO-EV W D BACH
PO BOX 12211
RESEARCH TRIANGLE PARK NC 27709

US ARMY RSRCH LAB
ATTN AMSRD-ARL-RO-MM J LAVERY
PO BOX 12211
RESEARCH TRIANGLE PARK NC 27709-2211

US ARMY RSRCH LAB
ATTN AMSRD-ARL-CI-OK-T TECHL PUB (2 COPIES)
ATTN AMSRD-ARL-CI-OK-TL TECHL LIB (2 COPIES)
ATTN AMSRD-ARL-D J M MILLER
ATTN AMSRD-ARL-SE J PELLEGRINO
ATTN AMSRD-ARL-SE S VINCI
ATTN AMSRD-ARL-SE-RE B ROD
ATTN AMSRD-ARL-SE-RL M DUBEY
ATTN AMSRD-ARL-SE-RM
A SINDORIS
ATTN AMSRD-ARL-SE-S J EICKE

US ARMY RSRCH LAB (cont'd)
ATTN AMSRD-ARL-SE-S M KOLODNY
ATTN AMSRD-ARL-SE-S R SARTAIN
ATTN AMSRD-ARL-SE-SA C REIFF
ATTN AMSRD-ARL-SE-SA
D ROBERTSON
ATTN AMSRD-ARL-SE-SA H VU
ATTN AMSRD-ARL-SE-SA J HOUSER
ATTN AMSRD-ARL-SE-SA J PRICE
ATTN AMSRD-ARL-SE-SA K BENNETT
ATTN AMSRD-ARL-SE-SA
L ISAIAH-WEATHERS
ATTN AMSRD-ARL-SE-SA L SIM
ATTN AMSRD-ARL-SE-SA
L SOLOMON
ATTN AMSRD-ARL-SE-SA
M SCANLON
ATTN AMSRD-ARL-SE-SA N SROUR
ATTN AMSRD-ARL-SE-SA
R DAMARLA
ATTN AMSRD-ARL-SE-SA R FRANKEL
ATTN AMSRD-ARL-SE-SA S TENNEY
ATTN AMSRD-ARL-SE-SA T PHAM
ATTN AMSRD-ARL-SE-SA
T TRAN-LUU

US ARMY RSRCH LAB (cont'd)
ATTN AMSRD-ARL-SE-SE D HULL
ATTN AMSRD-ARL-SE-SE G FISCHER
ATTN AMSRD-ARL-SE-SE
J BURNETTE
ATTN AMSRD-ARL-SE-SE
J DAMMANN
ATTN AMSRD-ARL-SE-SE J FINE
(10 COPIES)
ATTN AMSRD-ARL-SE-SE M THIELKE
ATTN AMSRD-ARL-SE-SE
N NASRABADI
ATTN AMSRD-ARL-SE-SE
P GILLESPIE
ATTN AMSRD-ARL-SE-SS
A EDELSTEIN
ATTN AMSRD-ARL-SE-SS A LADAS
ATTN AMSRD-ARL-SE-SS D GILL
ATTN AMSRD-ARL-SE-SS
D THOMPSON
ATTN AMSRD-ARL-SE-SS J CHOPACK
ATTN IMNE-ALC-IMS MAIL &
RECORDS MGMT
ADELPHI MD 20783-1197